are used in the algorithm. A surface of $\xi =$ constant and $\zeta =$ constant cell faces is tagged for ξ line insertion if the average divergence exceeds a specified tolerance:

$$\frac{1}{j_{\max}} \sum_{j=1}^{j\max} (\Delta)_j > \beta_{\text{avg}} \tag{4}$$

Similarly, a surface of $\xi =$ constant and $\zeta =$ constant cell faces is tagged for ξ line insertion if the maximum divergence exceeds a specified tolerance:

$$\max_j (\Delta)_j > \beta_{\max} \tag{5}$$

where $\beta_{\max} > \beta_{\text{avg}}$. The line insertion occurs at the midpoints of the cell faces.

Sample Grids

We now include two sample grids to illustrate the general properties of the method. Figure 2 shows the symmetry plane and a spanwise surface for a grid generated around an M6 wing. Figure 3 shows surfaces of a grid generated for an "X-38-like" configuration. In both cases line deletion produces a transition from a relatively dense body grid to a much coarser, more isotropic grid at the boundaries without the clustering of grid lines emanating from concave regions that is characteristic of grids generated using marching methods.

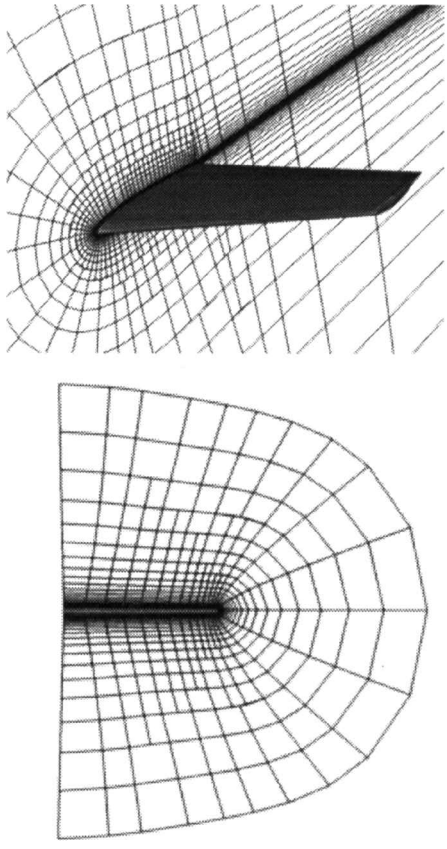

Fig. 2 Symmetry plane and spanwise surface of grid for M6 wing.

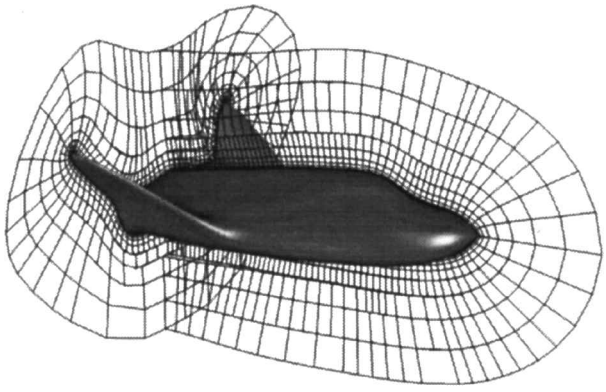

Fig. 3 Symmetry plane and exit surface of grid for X-38-like body.

Conclusions

The capability to generate semistructured, three-dimensional, hexahedral-dominant grids has been demonstrated. The method was shown to generate quality volume grids for surfaces with concave and convex regions. Although the parabolic marching method generates the grid in structured layers, this structure is lost at the interface between layers where a line-deletion/insertion algorithm based on cell aspect ratio and grid line divergence was applied. This strategy is not unique, and great flexibility exists in the definition of the deletion/insertion algorithm.

References

[1] Thompson, J. F., Soni, B. K., and Weatherill, N. P. (eds.), *Handbook of Grid Generation*, CRC Press, Boca Raton, FL, 1998.

[2] Shaw, J. A., "Hybrid Grids," *Handbook of Grid Generation,* edited by J. F. Thompson, B. K. Soni, and N. P. Weatherill, CRC Press, Boca Raton, FL, 1998, pp. 23.1–23.18.

[3] Kallinderis, Y., "Hybrid Grids and Their Applications," *Handbook of Grid Generation,* edited by J. F. Thompson, B. K. Soni, and N. P. Weatherill, CRC Press, Boca Raton, FL, 1998, pp. 25.1–25.18.

[4] Nakamura, S., "Marching Grid Generation Using Parabolic Partial Differential Equations," *Numerical Grid Generation*, edited by J. F. Thompson, Elsevier, New York, 1982, pp. 775–786.

[5] Noack, R. W., and Anderson, D. A., "Solution-Adaptive Grid Generation Using Parabolic Partial Differential Equations," *AIAA Journal*, Vol. 28, No. 6, 1990, pp. 1016–1023.

[6] Thompson, D. S., and Soni, B. K., "Semistructured Grid Generation in Three Dimensions Using a Parabolic Marching Scheme," AIAA Paper 2000-1004, Jan. 2000.

J. Kallinderis
Associate Editor

Evaluation of Finite Element Predictions of Analog Specimen Residual Stress Bondline Failures

David E. Richardson,* Bradley R. Hoskins,†
and Russell A. Crook‡
Thiokol Propulsion, Brigham City, Utah 84302-0707

Introduction

DEPENDING on the bonded system, manufacturing-induced bondline residual stresses can have a significant influence on the integrity of the system. There is a need for accurate and verifiable analytical techniques that can be used in the evaluation of bondline residual stresses. This Note will cover the testing and analyses that have been done with an analog cone residual stress specimen. The goal of this Note is to show that analytical predictions of bondline residual stress failures can be made with accuracy. To show the validity of the analyses, comparisons of the predicted failure times with the actual failure times are made.

This effort was initiated because significant work has been recently conducted to understand the effects of residual stresses on the

Presented as Paper 98-1945 at the AIAA/ASME/ASCE/AHS/ASC 39th Structures, Structural Dynamics, and Materials Conference, Long Beach, CA, 20–23 April 1998; received 7 August 2000; revision received 20 August 2000; accepted for publication 20 August 2000.

* Staff Engineer, Nozzle Design Engineering.
† Senior Engineer, Nondestructive Test Engineering.
‡ Senior Engineer, Adhesives Materials and Processes.

Table 1 Predicted times to failure

Specimen no.	Bond load, kN	Actual temperature, °C	Actual failure times	Finite element predicted stress, MPa	Finite element predicted failure time
1	44.5	32	2–3 min	14.5	2.5 min
2	40.0	34	20–60 min	13.0	2.3 min
3	35.6	32	2–8 h	11.6	19 min
4	26.7	33	2–4 h	8.69	3.6 h
5	17.8	38	8–10 days	5.72	1.6 days
6	17.8	41	1–2 h	5.72	13 h
7	44.5	22	1–2 h	17.4	50 min

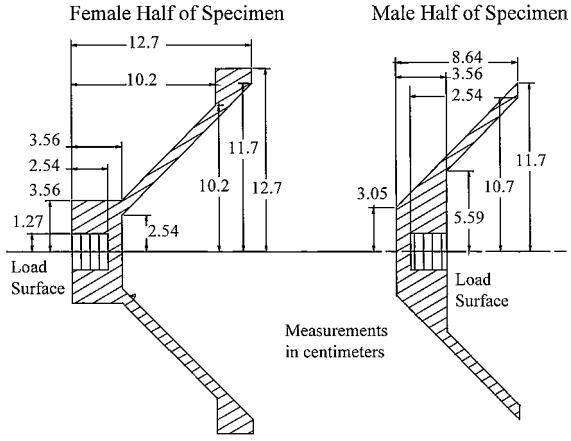

Fig. 1 Analog residual stress specimen geometry.

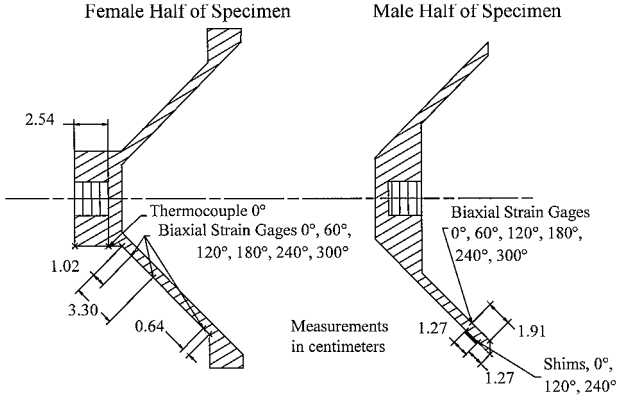

Fig. 2 Analog residual stress specimen instrumentation.

integrity of bondlines in the space shuttle's reusable solid rocket motor (RSRM) nozzles. For this program, several techniques have been developed for the analysis of bondline residual stresses.[1] These analysis techniques can be generalized for many other bonded structures.

These bondline residual stress analyses, however, have not been trivial due to several complexities. Of particular difficulty is that the constitutive and failure properties of the RSRM nozzle adhesives (and many other adhesives) are time and temperature dependent.[2,3] The strength of the RSRM adhesive under a sustained load is much less than that under standard test conditions and is very sensitive to small changes in temperature. Depending on the load source, these residual stresses can be three dimensional in nature.

Test Specimen

The tests described in this Note were accomplished using the conical specimen geometry with two aluminum adherends as seen in Fig. 1, with the strain gauge instrumentation noted in Fig. 2. The strain gauges were placed on the specimen in locations such that indications of failure could best be obtained. The locations of these strain gauges were determined by evaluating axisymmetric finite element analysis predictions of changes in strain with generic axisymmetric unbonds (techniques similar to those described in subsequent paragraphs). Gauges were placed in regions of both high- and low-strain gradients, so that the maximum effect of unbonding could be noted (regions of high-strain gradient) and so that the general response could be evaluated (regions of low-strain gradient).

Test Description

The bonding and testing of the conical specimens were conducted together in a continuous series of steps in a single environmental chamber. A hydraulic load press was placed inside the chamber for use during the mating of the adherends in the bonding process. The environmental chamber was used to control the cure temperature (40°C). After cure, the load that had been imposed on the specimen during cure was removed. The temperature of the environmental chamber was also changed from the cure temperature to the final constant test temperature. The bond loads used during cure and final test temperatures used after cure for the test program can be seen in Table 1.

Before bonding, the bond surfaces were cleaned, and primer was applied. After the primer had dried, adhesive shims were carefully bonded to the male half of the conical specimens in the locations specified in Fig. 2. The precured shims were used in the bonding process to ensure that a bond gap between adherends was obtained. The male half of the test specimen was placed on the load fixture, and the bond surfaces of the male and female specimens were first whetted with the adhesive EA946.

After attaching the female half of the specimen to the load fixture, the two halves were mated with a prescribed bonding load. As the parts were mated, the housings deflected both near the precured shims and near the load point. Next, each specimen was heated to the cure temperature (40°C). The cure temperature was maintained throughout the required cure time. The mating load was not released before or during the adhesive cure process; therefore, the specimens were cured with the adherends in this deflected (or prestressed) state. After the adhesive was cured, the temperature of the specimens was changed from the cure temperature (40°C) to the final test temperature (Table 1). Next, all constraints and the mating load were removed so that the adherends were allowed to spring back toward their unstressed condition. Because of the presence of the cured adhesive, the adherends could only spring to an intermediate position that was in an equilibrium condition with the adhesive. This spring-back action is what induced the residual stresses in the specimen bondlines. After release, the test specimens were maintained at the test temperature for several days so that the specimens would have time to experience residual stress-induced bondline failures. Strain gauges were monitored continuously.

Failure Identification

Strain gauges were used as the primary indicator of the bondline failure initiation time in the test specimens. As mentioned, the strain gauge locations (Fig. 2) were chosen to provide the best indications of failure. Because of the viscoelasticity of the adhesive, the strain gauges showed changes in measurements with time. Times when the trends of these strain changes altered unexpectedly were assumed to indicate failure. According to the viscoelastic material model, the adhesive reaches equilibrium within approximately 1 h at 30°C. Thus, significant strain movement after 1 h was also noted as an indication of failure. Ultrasonic scans were used to verify that failure

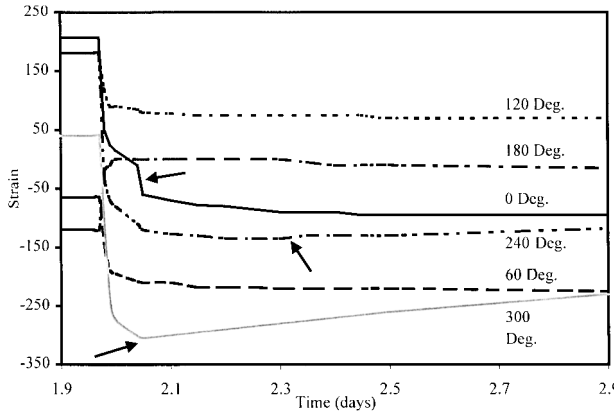

Fig. 3 Strain gauge data for specimen 3.

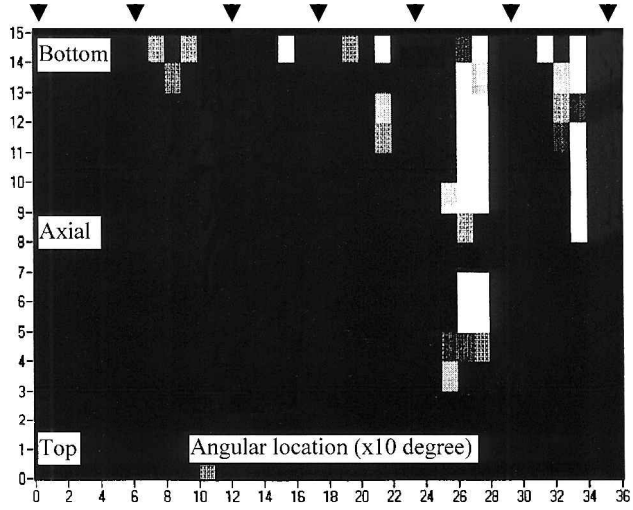

Fig. 4 Ultrasonic inspection of specimen 3.

occurred in the specimens and to evaluate the general location of the predicted unbonds.

An example of how the time of initiation of failure was determined can be seen in Fig. 3 for specimen 3. Note that at about 1.98 days from the initiation of the bonding process the specimen is released from the bond load. As would be expected, the strains in the housing change with time due to the viscoelastic nature of the adhesive (and/or failure). The three arrows in Fig. 3 mark assumed indications of failure. Note the change in strain from moving toward compression to moving toward tension for the 240- and 300-deg gauges and the abrupt change in strain magnitude for the 0-deg gauge (this 0-deg indication is possibly not an indication of failure but an artifact of unbonds at 300 deg). Given these indications, failure is assumed to have occurred at the angular locations between 240 and 360 deg with failure times between approximately 2 h (0-deg gauge) and approximately 8 h (240-deg gauge) after load release. Ultrasonic inspections were used to verify the presence of unbonds (Fig. 4).

Analysis Approach

The finite element evaluation of these analog cone test specimens was conducted with one analysis computer run using several different steps. Analytical techniques used in the analyses were similar to those used for analyses of the RSRM nozzle bondlines.[1] The following is a brief discussion of the approach that was used:

1) In the first analysis step, the female half of the specimen was forced with a generic bond load (27 kN) onto the precured adhesive shims on the male half of the specimen, forcing deformations of the adherends. This loading was applied at the cure temperature. The adhesive elements were forced to remain in a stress-free and strain-free condition during this step (using options available in the finite element code).

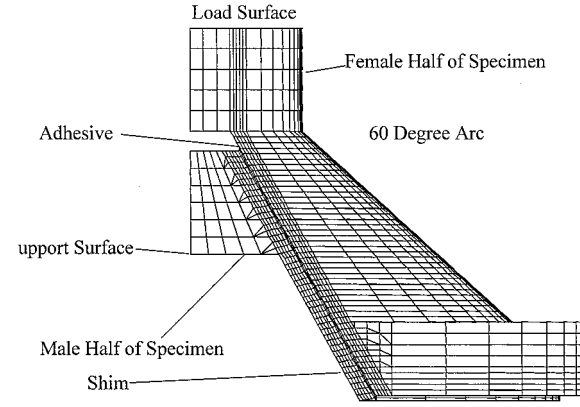

Fig. 5 Three-dimensional finite element grid for the residual stress specimen.

2) The parts were released to the final test temperature in the second step and subsequent steps. Final temperatures ranged from 20 to 40°C, depending on the test. The adhesive was locked to the housings, allowing residual stresses to be induced into the bondline as the adherends attempted to spring back to their stress-free condition.

On completion of the analyses, the resulting stresses and strains were scaled and interpolated as necessary to match the different test conditions (both load and temperature). Interpolation between analyses of different load and temperature combinations was assumed to be accurate for this evaluation.

Finite Element Model

All analyses were accomplished using the ABAQUS finite element code. The test specimens were modeled using the three-dimensional finite element model seen in Fig. 5. To simplify the model, symmetry was used. A finite element grid of only a 60-deg slice of the test specimen was created.

Linear solid elements were used to model the components of the test specimen. Because the housing slides along the shim surface during mating, gap elements were required to be used to model the interface between the shims and the bond surface of the female adherend (the shim was attached to the male adherend).

Material Model

The bondline adhesive (EA946) has been shown to have time- and temperature-dependent constitutive and failure properties. Analytical models of bond systems can be very complex. These models can be costly and require an unacceptably large amount of run time if the aforementioned material property time dependencies are included in the analyses. To simplify analyses of the RSRM nozzle bondline residual stresses, the adhesive was modeled using the equilibrium modulus (6.2 MPa) and a constant bulk modulus (1380 MPa). For this study, the adhesive was also modeled with these equilibrium material properties. This approximation is assumed adequate for analyses of the RSRM nozzle because the time of interest is well past the time required to reach equilibrium. For the analog specimens, this approximation is fair given that the majority of the analog tests were conducted at 30°C or higher. This is one of the major assumptions that required evaluation through the test data.

To provide a debonding failure model for the adhesive, extensive testing was also conducted to determine the time- and temperature-dependent nature of the failure properties of the adhesive EA946. Details of the failure model and the test data are not within the scope of this Note. A brief summary of key characteristics of the failure model and the testing is provided here so that a better understanding of the testing and analyses may be had. In some instances the capability of the adhesive under sustained loads can be less than half that seen in standard tensile tests. Because the glass transition temperature of the adhesive is so low, small changes in temperature lead to significant changes in capability in normal ambient temperature

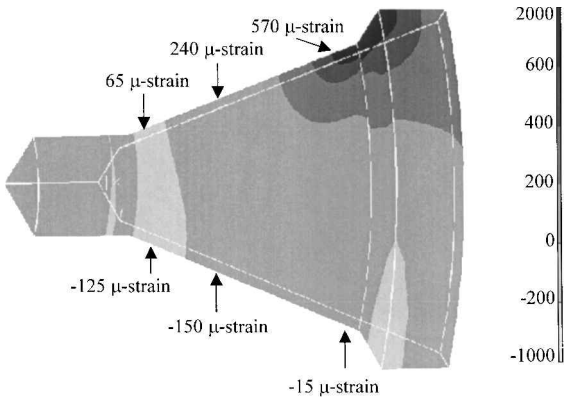

Fig. 6 Predicted vs measured hoop strain.

conditions (20–40°C). The model is also very sensitive to small changes in loading conditions. A simple power law model was developed to describe failure. The time/temperature shift is modeled with a Williams–Landel–Ferry-type (see Ref. 4) formula:

$$\sigma_f = N_\beta (t_f / a_T)^{-0.0986} \tag{1}$$

$$\log_{10}(a_T) = \frac{-C_1(T - T_0)}{C_2 + (T - T_0)} \tag{2}$$

where σ_f is failure stress (fit to average failure data), t_f is failure time, $N_\beta = 27.3$ MPa, a_T is the temperature/time shift factor, $C_1 = 36$, $C_2 = 252$, T is temperature, and $T_0 = 21$°C (reference temperature).

The model was developed by using poker chip adhesion test specimens. Not surprisingly, the test data exhibited a great deal of scatter in times to failure for a given load. The scatter is inherent in this type of test. Failure times in the constant load tests were seen to have full order of magnitude range of scatter. For example, poker chip specimens subjected to an average stress of 2 MPa and a temperature of 30°C had failure times ranging from 30 to 400 h. This range of scatter was seen in specimens subjected to many different loads and temperatures. Given the large amount of scatter in the experimental data under these controlled conditions, it was determined that predictions of failure in the analog specimens would be considered successful if the predictions were within an order of magnitude of the actual failure. It is, however, recommended that this scatter in failure times be taken into account when designing bond systems. In the RSRM program statistical methods are used to ensure that a conservative prediction of failure is made. Because of the scatter in the data, statistical approaches lead to extreme conservatisms. The intent of this Note is not to address these statistical methods, but to evaluate the prediction of average failure and to provide an evaluation of the analytical tools.

Results and Discussion

An example of the strain gauge predictions vs the actual measurements can be seen in Fig. 6. These predictions are good considering the size of the gauges and the accuracy of the placement. The finite element analysis predicted maximum bondline stresses were used to make estimates of failure times using Eqs. (1) and (2). It was assumed that if the actual failure times could be predicted that the finite element stress calculations and failure model are both validated. Table 1 contains a summary of these predicted failure times compared with the actual observed times to failure indications.

The predicted times to failure for specimens 1, 4, and 7 are very good. Predictions for specimens 2, 3, 5, and 6 are good because they are within an order of magnitude. These predictions are reasonable considering scatter in failure test data noted earlier. Samples 5 and 6 give an indication of the high sensitivity to temperature. Small changes in temperature can lead to significant change in failure times. The failure model is also very sensitive to small changes in load. As discussed, these failure time predictions that are within an order of magnitude are considered good.

Conclusions

As seen earlier, analytical techniques are available for evaluation of bondline residual stresses induced during manufacturing processes. Significant approximations of time- and temperature-dependent constitutive and failure properties were utilized to simulate the approach that would be required for much more complex geometric structures, for example, analyses of the RSRM nozzle. The intent of the study was to evaluate the accuracy of these assumptions with an analog specimen and to study the utility of the analytical techniques for use as a design tool.

The analog cone residual stress test specimens described herein are valuable tools in providing test data for evaluation of these residual stress evaluation techniques. The specimen design provides for the use of strain gauges to monitor the failure initiation and allows for the use of ultrasonic inspection for validation of failure indications.

The correlation of test data with analysis predictions seen in this Note indicates that a good analytical tool has been developed for predictions of failures caused by residual stresses in analog specimens. Failure predictions can be made with good accuracy (within an order of magnitude). Failure times in the residual stress analog specimens (as was noted with samples 5 and 6) and in actual bonded parts are expected to have a significant amount of scatter given that scatter in standard test specimens is great. Thus, care should be taken when using this EA946 adhesive (or any other similar adhesive with a room temperature glass transition temperature).

The analytical tools demonstrated in this Note can be very valuable for defining methods for controlling residual stresses in manufacturing and transportation conditions for actual bonded systems. These tools have led to vast improvements in RSRM nozzle processing. When using these residual stress analytical techniques in design or for process modifications, it is extremely important to give consideration to this variation in failure time. Statistical evaluations are required to ensure conservative assessments are made.

References

[1]Richardson, D. E., Crook, R. A., and Phipps, B. E., "Analyses of Manufacturing Residual Stresses in the Shuttle Redesigned Solid Rocket Motor Nozzle," *JANNAF Interagency Propulsion Committee, Rocket Nozzle Technology Sub-Committee Meeting*, Chemical Propulsion Information Agency Publ. 605, Columbia, MD, 1993, pp. 155–163.

[2]Richardson, D. E., and Crook, R. A., "Notes on Constitutive Property Changes Due to Nonlinearities and Pose Cure Aging for EA946 Adhesive," *JANNAF Interagency Propulsion Committee, Rocket Nozzle Technology Sub-Committee Meeting*, Chemical Propulsion Information Agency, Publ. 649, Columbia, MD, 1996, pp. 33–47.

[3]Richardson, D. E., Palumbos, A. V., Hoskins, B. R., and Lewis, T. J., "Verification of Finite Element Predictions of Residual Stress Bondline Failures in a Full-Scale Test Article," AIAA Paper 99-1413, April 1999.

[4]Ferry, J. D., *Viscoelastic Properties of Polymers*, Wiley, New York, 1980.

G. A. Kardomateas
Associate Editor